VERY-WIDE ELECTROTHERMAL TUNING OF GRAPHENE NANOELECTROMECHANICAL RESONATORS

Fan Ye[*], *Jaesung Lee, and Philip X.-L. Feng*[*]
Department of Electrical Engineering & Computer Science, Case School of Engineering,
Case Western Reserve University, Cleveland, OH 44106, USA
[*]Emails: fan.ye@case.edu; philip.feng@case.edu

ABSTRACT

We report on the first demonstration of electrothermally tunable graphene nanoelectromechanical resonators via Joule heating. We fabricate single-, bi- and tri-layer graphene resonators (up to 136MHz) to study electrothermal effects on resonance characteristics. The tri-layer graphene resonator exhibits frequency upshift from 9.5MHz to 26.1MHz by electrothermal heating, resulting in tuning range up to 180%. The device temperature is carefully verified via anharmonic frequency shift of Raman modes, exhibiting temperature elevation up to 600K in tri-layer graphene device with Joule heating. This work proves that electrothermal effects could broadly tune graphene resonators with high efficiency.

INTRODUCTION

Graphene, the forerunner of two-dimensional (2D) materials, has been employed as atomically thin building blocks for new nanoelectromechanical systems (NEMS) and has shown attractive potential for nanoscale actuators and sensors [1]. Compared to other 2D materials, graphene processes excellent electrical properties, such as extremely high mobilities at both room temperature (μ~140,000 $cm^2V^{-1}s^{-1}$) and low temperature (μ~1,000,000 $cm^2V^{-1}s^{-1}$) [2], and outstanding mechanical properties including very high Young's modulus (E_Y~1TPa) and superior strain limits (ε_{limit}~25%) [3]. Given these properties, graphene resonators have been demonstrated by using photothermal excitation [4] and electrostatic actuation [5] schemes. Moreover, graphene also possesses high temperature stability [6] and negative thermal expansion coefficient [7], hence graphene resonators should be inherently suited for, and may exhibit even better performance, at elevated temperatures. Graphene transistors are sometimes exposed to high temperature, by using furnace annealing or localized Joule heating, to clean and remove surface adsorbates or residues [5] after device fabrication. On-device *in-situ* high temperature operation of resonant graphene NEMS, however, has not been demonstrated yet.

In this work, we fabricate single-, bi-, and tri-layer (1L, 2L, and 3L) graphene resonators, and some of their arrays, by employing techniques including both specially designed stencil mask metal electrode deposition and all-dry transfer on pre-patterned electrodes, and investigate their resonance characteristics upon Joule heating. We use DC voltage to heat up graphene resonators, and apply AC/RF signal to excite resonance motions. We then simultaneously measure temperature and resonance characteristics of graphene resonators, in a custom-built Raman spectroscopy integrated in a laser interferometry motion detection system. We find in a 2L graphene resonator, the fundamental-mode resonance frequency shifts up from 80.1MHz to 86MHz ($\Delta f/f \approx 7.5\%$) with Joule heating. In a 3L graphene resonator, fundamental frequency elevates from 9.5MHz to 26.1MHz, demonstrating a very wide frequency tuning, up to $\Delta f/f \approx 180\%$. The temperature variations are simultaneously monitored by using Raman spectroscopy. We show resonant operations at elevated temperatures, in the range of 300K to 600K.

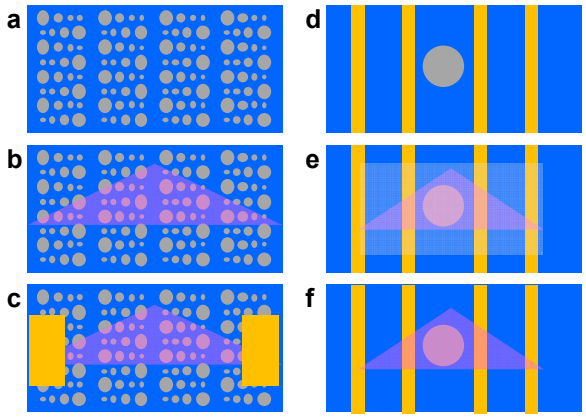

Figure 1: Illustration of two fabrication methods employed in this work. Method 1: (a) pre-patterned substrate with arrays of holes; (b) exfoliation of graphene flakes onto the substrate; (c) metal electrode deposition onto the graphene flakes using stencil masks. Method 2: (d) pre-patterned substrate with a microtrench and electrodes; (e) aligned dry stamp transfer of graphene onto substrate; (f) graphene flake covers the microtrench after lifting-up the PDMS stamp.

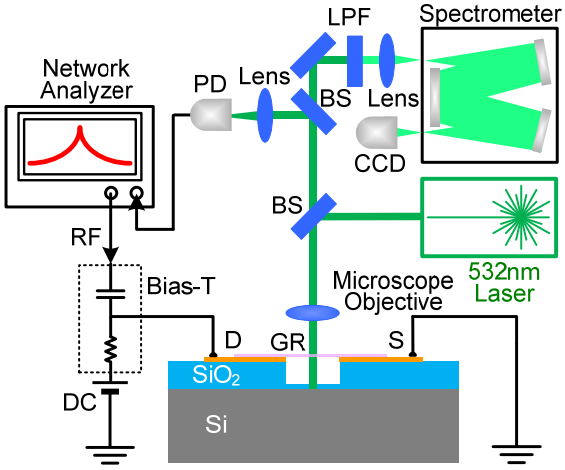

Figure 2: Measurement system with Raman spectroscopy and optical interferometry combined. LPF, PD, and BS are long-pass filter, photodetector & beam splitter, respectively.

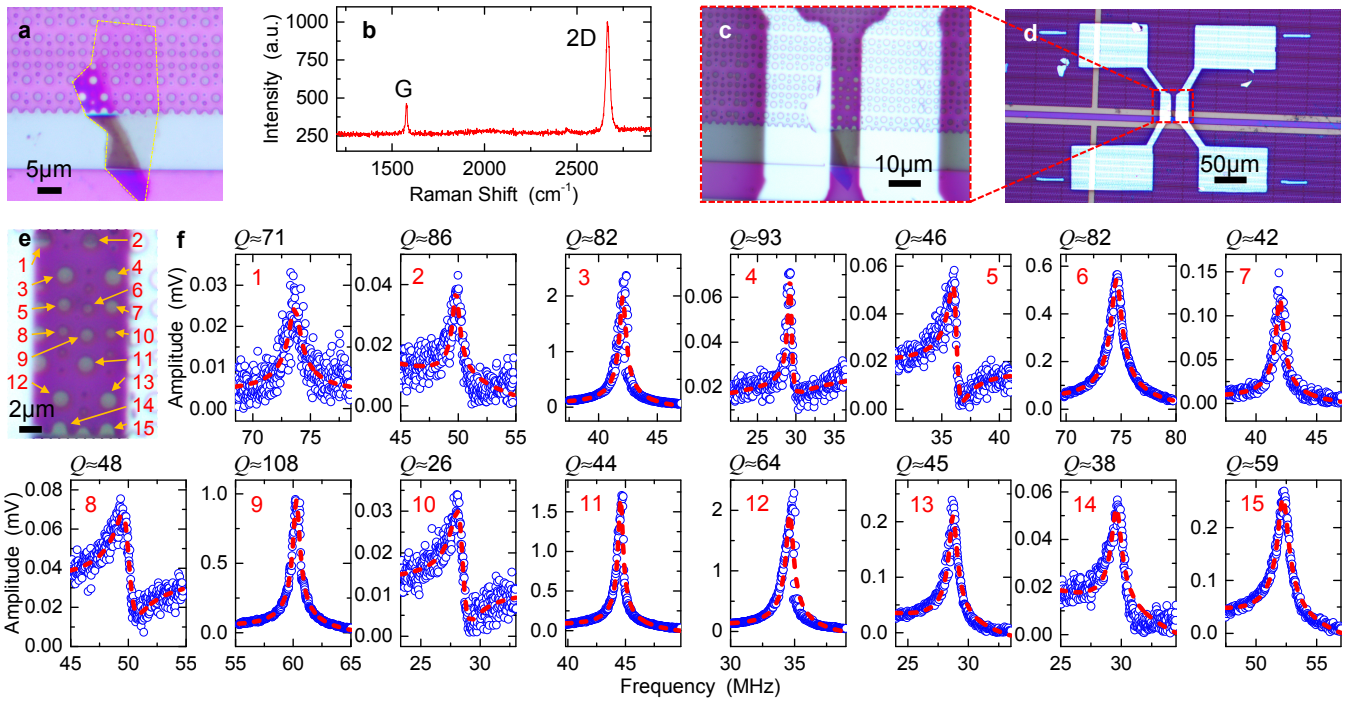

Figure 3: Measured resonances from an array of 1L graphene resonators. (a) Optical microscope image of exfoliated graphene flake and an array of 1L drumheads. (b) Raman spectrum of the 1L flake. (c)-(e) Optical images of 1L devices after metal deposition. (f) Resonances of the individual 1L devices in the array. Red numbers represent device IDs labeled in (e).

EXPERIMENTAL TECHNIQUES

We employ two different fabrication methods. For the 1L and 2L graphene devices and their arrays, we directly exfoliate graphene flakes on pre-patterned substrates with arrays of circular holes (Fig. 1a). After exfoliation, we use specially designed stencil masks to selectively deposit gold (Au) on two ends of the chosen graphene flake for making source and drain electrodes, to avoid contaminating devices. For the 3L graphene resonators, we use an all-dry stamp transfer method. Graphene flakes are first exfoliated on a PDMS stamp and then transferred to pre-patterned substrates with microtrenches and Au electrodes (see Fig. 1d-f).

We measure graphene resonances using an ultrasensitive laser interferometry system (Fig. 2). We excite resonance motions by using AC/RF voltage, supplied by the output signal from a network analyzer. A 532nm continuous waveform (CW) laser is focused, using a 50× microscope objective, on the center of the suspended graphene devices to detect the resonant motions. To avoid laser heating, laser power is limited below ~300μW, with a laser spot size of ~1μm. Motional optical responses from the graphene devices are transduced into electronic signals via a sensitive photodetector, and recorded by the same network analyzer.

Raman spectroscopy, which is integrated into the optical interferometric resonance measurement system (Fig. 2), is simultaneously performed during the Joule heating and electrothermal tuning measurement. Graphene devices are preserved in a vacuum chamber with an optical window. Raman scattered light from the graphene sample is collected in backscattering geometry and then guided to a spectrometer with a 1200g/mm grating configuration, through a series of optical components. The Raman signal is recorded using a liquid-nitrogen-cooled charge-coupled device (CCD). The spectral resolution of our Raman system is ~1 cm^{-1}. Typical measurement range is 1200 to 3000 cm^{-1}, to mainly observe the D, G, and 2D graphene Raman modes (peaks).

RESONANCE MEASUREMENTS

Figure 3a to 3e show optical microscope images of the 1L devices and their Raman signatures. With stencil mask metal deposition, we fabricate an array of 15 1L graphene drumhead devices with shared source and drain electrodes. Diameters of devices are ~1μm, ~1.25μm, and ~1.5μm. We refer these devices from Device #1 to #15 (Fig. 3e); and the resonances measured from them are shown in Fig. 3f. Resonances of the 15 devices vary from 25MHz to 80MHz with quality (Q) factors of 26 to 108 (at 300K), depending on device sizes and pre-tension levels. Similar to the 1L arrays, we fabricate arrays of 2L graphene resonators with diameters of 1μm, 1.25μm, and 1.5μm (Fig. 4a to 4e). Resonances of these 15 devices are at 66MHz to 136MHz with Qs of 118 to 400, as shown in Fig. 4f. Some of these devices, *e.g.*, # 3, #5, #7, #9 and #14, exhibit clear multimode resonances.

The 3L device shown in Fig. 5 is fabricated using the aligned all-dry transfer method; and its diameter is ~5μm. With small DC (V_{DC}=0.5V) and AC (V_{AC}=0.02V) voltages applied across source and drain electrodes, the temperature of the device remains at near room temperature (~300K), as confirmed by Raman spectroscopy results; and the device exhibits a resonance frequency of ~9.5MHz with Q ~ 83.

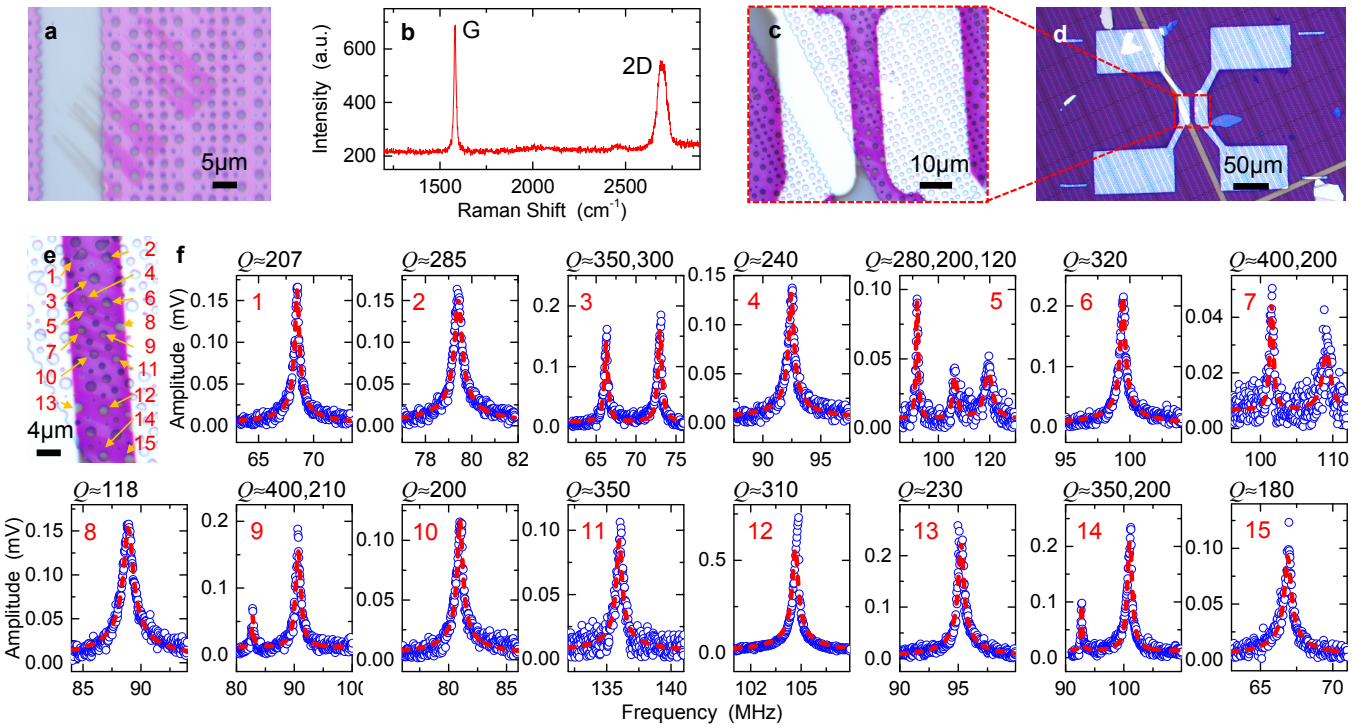

Figure 4: Measured resonances from an array of 2L graphene resonators. (a) Optical microscope image of 2L graphene flakes. (b) Raman response of the 2L graphene flake. (c)-(e) Optical microscope images of 2L devices after deposition of metal electrodes through a stencil mask. (f) Measured resonances of the 15 2L graphene devices. Device IDs are labeled in (e).

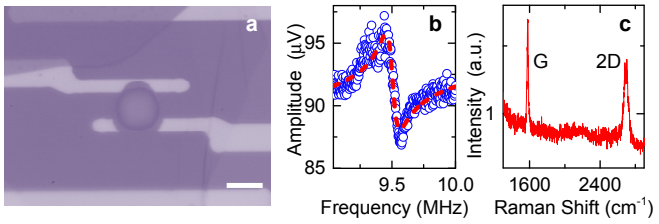

Figure 5: A 3L graphene resonator. (a) Optical microscope image of the 3L graphene device (scale bar: 5μm). (b) Measured resonance and (c) Raman signal of the device.

ELECTROTHERMAL TUNING

We examine resonance frequency tuning by using a DC bias voltage to control Joule heating electrothermal effects on the graphene resonators together with a small AC/RF bias to excite the resonance motions. Resonance characteristics and device temperatures are simultaneously monitored using the combined optical interferometry and Raman spectroscopy measurement system depicted in Fig. 2.

Resistance of the 1L array in Fig. 3 is larger than 1MΩ (due to a defective wire-bonding), making Joule heating less effective and electrothermal tuning weak in this 1L array. Resistance of the 2L device is relatively small (2.3kΩ), exhibiting obvious frequency tuning, as shown in Fig. 6. In 2L Device #8 (see Fig. 4e), as applied DC bias voltage increases from 0.7V to 2.5V, we observe a frequency upshift from 80.1MHz to 86MHz. Due to unique negative thermal expansion coefficient of graphene, Joule heating introduced by applied V_{DC} yields additional tension in the device, which leads to frequency upshift. We note that the amplitude of the resonance is also enhanced as V_{DC} increases. This could be attributed to generated electrothermal force from Joule heating. As the strength of the electrothermal driving force is closely related to both V_{DC} and V_{AC}, higher V_{DC} leads to larger driving force, boosting the resonance motions. Duffing nonlinearity in the 2L Device #8 (see Fig. 4e) is also demonstrated — we find that the electrothermal excitation is very efficient, able to drive resonator into deep nonlinear regime with relatively small V_{DC} and V_{AC} (Fig. 7).

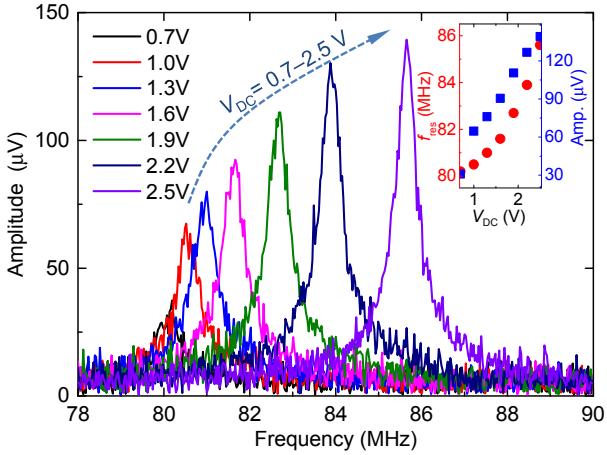

Figure 6: Frequency tuning in a 2L graphene resonator as DC bias voltage increases from 0.7V to 2.5V. Inset shows frequency and amplitude responses with increasing V_{DC}.

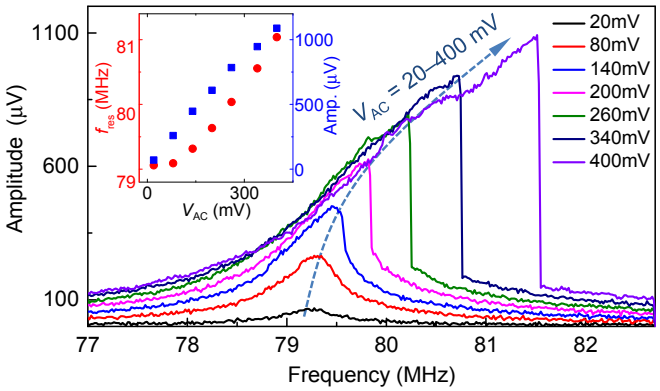

Figure 7: Measured Duffing nonlinear response in a 2L graphene resonator (Device #8) as V_{AC} increases from 20mV to 400mV with constant V_{DC} = 1V. Inset: frequency and amplitude dependency on varying applied V_{AC}.

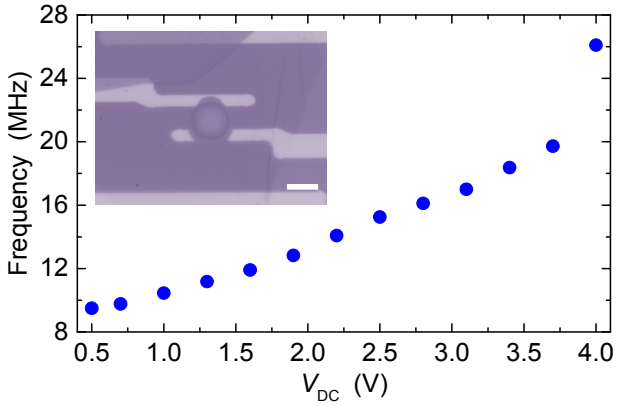

Figure 8: Frequency tuning in 3L graphene device as DC voltage increases from 0.5V to 4.3V. Inset shows an optical microscope image (scale bar: 5μm).

We further study electrothermal tuning on the 3L device shown in Fig. 5. Its resonance frequency increases from 9.5MHz to 26.1MHz with V_{DC} sweeping from 0.5V to 4.3V, exhibiting a frequency tuning range up to 180% (Fig. 8). This very wide frequency tuning can be attributed to a combination of several aspects: the 3L device has low contact resistance between graphene and Au electrodes; injecting larger electrical power into the device; larger device dimensions compared with the 1L and 2L devices, reducing heat dissipation and leading to higher temperature operation.

DEVICE TEMPERATURE CALIBRATION

We measure Raman spectra during Joule electrothermal heating and estimate temperature of the graphene resonators. We find that as V_{DC} increases, due to anharmonic effects from high temperature, both G peak and 2D peak shift to the low wave number. In addition, thermal emission becomes pronounced under high V_{DC}, resulting in higher background level of the Raman spectra. By fitting Raman peaks with Lorentzian function, we extract peak positions for both G peak and 2D peak, and estimate temperature of graphene crystal from the peak shifts. Since 2D peak becomes much boarder at high temperature, we use G peak position to obtain the device temperature. As V_{DC} increases to 4.0V, the temperature increases from 300K up to 600K (Fig. 9).

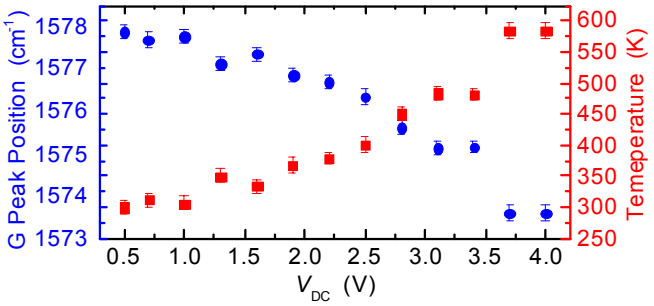

Figure 9: Measured graphene Raman G peak position and calibrated device temperature as at various V_{DC} levels.

CONCLUSIONS

In summary, we have demonstrated Joule heating and electrothermal tuning of high frequency graphene resonators. The 1L and 2L graphene devices are fabricated using stencil mask metal deposition, and the 3L device is fabricated using the dry-transfer method. In the 2L device, frequency increases from 80.1MHz to 86MHz. In the 3L device, frequency increases from 9.5MHz to 26.1MHz, with tuning range up to 180%. Raman spectroscopy shows that the temperature of 3L device elevates from 300K to 600K. These results suggest new possibilities of building widely electrically tunable resonant graphene NEMS.

ACKNOWLEDGEMENTS

We thank financial support from the National Academy of Engineering (NAE) Grainger Foundation Frontier of Engineering (FOE) Award (FOE2013-005), and the National Science Foundation through CAREER Award (Grant ECCS-1454570) and CCSS Award (Grant ECCS-1509721). We thank Rui Yang for help in the early stage device fabrication.

REFERENCES

[1] J. Lee, P. X.-L. Feng, in *Proc. IEEE Int. Freq. Contr. Symp. (IFCS 2012)*, pp. 1-7, DOI: 10.1109/FCS.2012.6243742, Baltimore, MD, USA, May 21-24, 2012.

[2] L. Wang, I. Meric, P. Y. Huang, Q. Gao, Y. Gao, H. Tran, T. Taniguchi, K. Watanabe, L. M. Campos, D. A. Muller, J. Guo, P. Kim, J. Hone, K. L. Shepard, C. R. Dean, *Science,* vol. 342, pp. 614-617, 2013.

[3] C. Lee, X. Wei, J. W. Kysar, J. Hone, *Science,* vol. 321, pp. 385-388, 2008.

[4] J. S. Bunch, A. M. van der Zande, S. S. Verbridge, I. W. Frank, D. M. Tanenbaum, J. M. Parpia, H. G. Craighead, P. L. McEuen, *Science,* vol. 315, pp. 490-493, 2007.

[5] C. Chen, S. Rosenblatt, K. I. Bolotin, W. Kalb, P. Kim, I. Kymissis, H. L. Stormer, T. F. Heinz, J. Hone, *Nature Nanotechnology,* vol. 4, pp. 861-867, 2009.

[6] A. A. Balandin, S. Ghosh, W. Bao, I. Calizo, D. Teweldebrhan, F. Miao, C. N. Lau, *Nano Letters,* vol. 8, pp. 902-907, 2008.

[7] D. Yoon, Y.-W. Son, H. Cheong, *Nano Letters,* vol. 11, pp. 3227-3231, 2011.